

Exploring the Variation Quantum Eigensolver: through an application in the Lipkin Model

Keran Chen

(Dated: June 23, 2023)

This report is a study on the Variational Quantum Eigensolver, with a focus on theory, its implementation and a comparison of its performance on the different model to that of a high-level library, classical eigensolvers and exact solutions. The results are optimistic for the various models. Most of the time our implementation had results comparable to the result from using VQE in Qiskit, even though there was some discrepancy in finding the ground state energy for the Lipkin Model $J = 2$. We concluded that it should be reasonably solved by trying different classical optimisation methods, experimenting with ansatzs and initialisations of the parameters.

I. INTRODUCTION

The development of quantum computing presents an alternative ways to simulate quantum problems. Among various applications of quantum computing, its potential in simulating quantum many-body systems with the Variational Quantum Eigensolver (VQE) is one of the promising near-term application we can achieve. [1]

The study of quantum many-body systems has been a fundamental aspect of quantum physics. Understanding these systems requires the ability to model the system and solve the Hamiltonian. Finding the ground state energy in a given Hamiltonian is one of the most essential problem to, for instance, condensed matter physics. It is, however, also a task that is computationally intensive, particularly as the system size grows. The VQE method, an algorithm that combines both classical and quantum schemes, promises the potential for solving complex systems with polynomial time. [1] Inspired by Hlatshwayo's article on *simulating excited states of Lipkin model on a quantum computer* [2], this study is heavily focused on trying to study the Lipkin model.

The Lipkin-Meshkov-Glick (LMG) model, or Lipkin model for short, is one of the paradigms for studying quantum many-body physics. It is a relatively simple model consist of N fermions in a two level system with N degeneracy. One of the advantage to the Lipkin model is that it can be easily expressed using the quasispin operators. [3]

This is a study of the fundamentals in quantum computations with the focus of implementing basic quantum circuits and the VQE methods for solving the Lipkin model with $J = 1$ and $J = 2$. We first implemented a fully functional quantum computer simulator which works similar to qiskit, then implemented the VQE methods and compare the results obtained by numerical eigensolvers and the VQE class from qiskit. For the application, we started by solving a simple one qubit system then a two qubit system. Through which we also computed the Von Neumann entropy and investigated the role of entanglement.

In the report, the theory of quantum computing and the models to which we will be applying the VQE are presented in Section II, after that are explanation of the

methodology used in the simulations in Section III, including the mapping of the models, first choice of ansatz and measurements. This will be followed by presentation of results obtained during the simulations in Section IV and a discussion of the results thereafter in Section V, before finally concluding our findings in Section VI.

II. THEORY

We'll first describe the basics of quantum computing, followed by the models being studied and finally the VQE algorithm.

A. Quantum Computing

As an analogy to the classical "bits", the heart of quantum computer is "qubits". To distinguish them from "bits", we represent them as kets.

$$|0\rangle = \begin{pmatrix} 1 \\ 0 \end{pmatrix}, \quad |1\rangle = \begin{pmatrix} 0 \\ 1 \end{pmatrix}$$

These are also our computational basis for the one qubit system. As a convention, the computational basis are usually the eigenbasis for the Pauli Z operator, σ_z or Z , the latter is used for simplicity.

For multiple qubits, the computational basis is defined by tensor products of the single-qubit states, such as $|0\rangle \otimes |0\rangle$ as the 0 state for a two qubit (bipartite). The \otimes sign is often omitted, for example, the basis for a bipartite system are written as $|00\rangle$, $|01\rangle$, $|10\rangle$, and $|11\rangle$ for two qubits.

Quantum gates are operators that change qubit states in order to perform an operation. The ones that most essential to this article are listed below:

- X-gate (NOT gate): Maps $|0\rangle$ to $|1\rangle$ and vice versa. It's the Pauli-X matrix.

$$X|0\rangle = |1\rangle \tag{1}$$

$$X|1\rangle = |0\rangle \tag{2}$$

$$X = \begin{pmatrix} 0 & 1 \\ 1 & 0 \end{pmatrix} \quad (3)$$

- Y-gate: Flips the bit and multiplies the phase by i . It's the Pauli-Y matrix.

$$Y|0\rangle = i|1\rangle \quad (4)$$

$$Y|1\rangle = -i|0\rangle \quad (5)$$

$$Y = \begin{pmatrix} 0 & -i \\ i & 0 \end{pmatrix} \quad (6)$$

- Z-gate (phase-flip gate): Flips the phase of the $|1\rangle$ state. It's the Pauli-Z matrix.

$$Z|0\rangle = |0\rangle \quad (7)$$

$$Z|1\rangle = -|1\rangle \quad (8)$$

$$Z = \begin{pmatrix} 1 & 0 \\ 0 & -1 \end{pmatrix} \quad (9)$$

- Hadamard gate: Creates (maximum) entanglement.

$$H|0\rangle = \frac{1}{\sqrt{2}}(|0\rangle + |1\rangle) \quad (10)$$

$$H|1\rangle = \frac{1}{\sqrt{2}}(|0\rangle - |1\rangle) \quad (11)$$

$$H = \frac{1}{\sqrt{2}} \begin{pmatrix} 1 & 1 \\ 1 & -1 \end{pmatrix} \quad (12)$$

- S^\dagger (S-dagger or S-inverse): Applies a $-i$ phase shift to the $|1\rangle$ state.

$$S^\dagger|0\rangle = |0\rangle \quad (13)$$

$$S^\dagger|1\rangle = -i|1\rangle \quad (14)$$

$$S^\dagger = \begin{pmatrix} 1 & 0 \\ 0 & -i \end{pmatrix} \quad (15)$$

- Rotation gates. R_x , R_y gates rotate the qubit around the x and y axis of the Bloch sphere by θ respectively.

$$R_x(\theta)|\psi\rangle = e^{-i\frac{\theta}{2}X}|\psi\rangle \quad (16)$$

$$R_y(\theta)|\psi\rangle = e^{-i\frac{\theta}{2}Y}|\psi\rangle \quad (17)$$

where $|\psi\rangle$ is the initial state of the qubit and θ is the angle for the rotation.

- CNOT (Controlled NOT) gate: Applies a NOT gate to the second qubit (target) only if the first qubit (control) is in the state $|1\rangle$.

$$CNOT = \begin{pmatrix} 1 & 0 & 0 & 0 \\ 0 & 1 & 0 & 0 \\ 0 & 0 & 0 & 1 \\ 0 & 0 & 1 & 0 \end{pmatrix} \quad (18)$$

- SWAP gate: This gate exchanges the states of two qubits.

$$SWAP = \begin{pmatrix} 1 & 0 & 0 & 0 \\ 0 & 0 & 1 & 0 \\ 0 & 1 & 0 & 0 \\ 0 & 0 & 0 & 1 \end{pmatrix} \quad (19)$$

The Von Neumann entropy is given by

$$S(A, B) = -\text{Tr}(\rho_{A,B} \log_2(\rho_{A,B})). \quad (20)$$

It measures the degree of entanglement of the system.

B. Simple Models

We studied the ground state energy for two simple Hamiltonians first. They can both be represented by

$$H = H_0 + \lambda H_1 \quad (21)$$

where H_0 is the non-interacting term, H_1 is the interacting term and λ is the interaction strength which takes values $[0, 1]$.

1. One-Qubit System

$$H = \begin{bmatrix} H_{11} & H_{12} \\ H_{21} & H_{22} \end{bmatrix},$$

$$H_0 = \begin{bmatrix} E_1 & 0 \\ 0 & E_2 \end{bmatrix}, \quad (22)$$

$$H_I = \begin{bmatrix} V_{11} & V_{12} \\ V_{21} & V_{22} \end{bmatrix}, \quad (23)$$

They can be rewrite using Pauli matrices (in order to do quantum computation with)

$$H_0 = \mathcal{E}I + \Omega Z, \quad \mathcal{E} = \frac{E_1 + E_2}{2}, \quad \Omega = \frac{E_1 - E_2}{2}, \quad (24)$$

and

$$H_I = cI + \omega_z Z + \omega_x X, \quad (25)$$

with $c = (V_{11} + V_{22})/2$, $\omega_z = (V_{11} - V_{22})/2$ and $\omega_x = V_{12} = V_{21}$. We choose $E_1 = 0$, $E_2 = 4$, $V_{11} = -V_{22} = 3$ and $V_{12} = V_{21} = 0.2$.

2. Two-Qubit System

$$H_0 = \begin{bmatrix} \epsilon_{00} & 0 & 0 & 0 \\ 0 & \epsilon_{10} & 0 & 0 \\ 0 & 0 & \epsilon_{01} & 0 \\ 0 & 0 & 0 & \epsilon_{11} \end{bmatrix} \quad (26)$$

$$H_I = H_x \sigma_x \otimes \sigma_x + H_z \sigma_z \otimes \sigma_z, \quad (27)$$

We choose $H_x = 2.0$, $H_z = 3.0$ and $\epsilon = [0.0, 2.5, 6.5, 7.0]$.

Rewrite H_0 in terms of the computational basis Z and I .

$$H_0 = aI \otimes I + bI \otimes Z + cZ \otimes I + dZ \otimes Z,$$

Solving the above equations, we get¹

$$a = 4, b = -0.75, c = -2.75, d = -0.5.$$

and using the gates we have to switch to the computational basis $Z \otimes I$ we have:

Let the swap gate be denoted by \mathcal{S} , and cnot gate with control on qubit 1 and target on qubit 0 be \mathcal{CN} .

$$H_0 = 4I \otimes I - 0.75(\mathcal{SZ} \otimes I\mathcal{S}) - 2.75Z \otimes I - 0.5(\mathcal{CN}(1,0)Z \otimes I\mathcal{CN}(1,0))$$

$$H_I = H_x \sigma_x \otimes \sigma_x + H_z \sigma_z \otimes \sigma_z,$$

Rewrite X into $I \otimes Z$

$$H_I = H_x(I \otimes \sigma_z)(\sigma_z \otimes I) + H_z(\sigma_z \otimes I)(I \otimes \sigma_z)$$

$$H_I = \lambda(H_x \mathcal{SZ} \otimes I\mathcal{S}) + \lambda(H_z \mathcal{CN}(1,0)Z \otimes I\mathcal{CN}(1,0))$$

$$\begin{aligned} H &= H_0 + H_I = 4I \otimes I \\ &\quad + (-0.75 + \lambda H_x)(\mathcal{SZ} \otimes I\mathcal{S}) \\ &\quad + -2.75 Z \otimes I \\ &\quad + (-0.5 + \lambda H_z)(\mathcal{CN}(1,0)Z \otimes I\mathcal{CN}(1,0)) \end{aligned}$$

C. Lipkin Model

According to the original paper, the Lipkin model was proposed to be simple enough to solve analytically, and yet non-trivial. “The model considers a situation where N fermions distributed in two levels each having an N -fold degeneracy and separated by an energy ϵ . Each described by a quantum number σ which has the value $+1$ in the upper shell and -1 in the lower shell, and a quantum number p specifying the particular degenerate state within the shell. For each value of p there are two corresponding states, one in the lower shell and one in the upper shell. Interactions can scatter these fermions in pairs between the 2 levels without changing the values of p . Let $a_{p\sigma}^\dagger$ be the creation operator for a particle in the p state of the σ level [3]. The Hamiltonian is given by

$$\begin{aligned} H_0 &= \epsilon J_z, \\ H_1 &= \frac{1}{2}V \sum_{p,p',\sigma} a_{p\sigma}^\dagger a_{p'\sigma}^\dagger a_{p'-\sigma} a_{p-\sigma}, \\ H_2 &= \frac{1}{2}W \sum_{p,p',\sigma} a_{p\sigma}^\dagger a_{p'-\sigma}^\dagger a_{p'\sigma} a_{p-\sigma}. \end{aligned} \quad (28)$$

In the lectures it was shown that the Lipkin Hamiltonian can be written as

$$\begin{aligned} H_0 &= \epsilon J_z, \\ H_1 &= \frac{1}{2}V (J_+^2 + J_-^2) \\ H_2 &= \frac{1}{2}W (-N + J_+ J_- + J_- J_+) \end{aligned} \quad (29)$$

where the J_+ , J_- are quasispin ladder operators, and J_z is the quasispin projection operator in the Z direction and the total Hamiltonian is

$$H = H_0 + H_1 + H_2.$$

$$1. \quad J = 1$$

Starting from relations involving the quasispin operators:

$$\begin{aligned} J_+ |J, J_z\rangle &= \sqrt{J(J+1) - J_z(J_z+1)} |J, J_z+1\rangle, \\ J_- |J, J_z\rangle &= \sqrt{J(J+1) - J_z(J_z-1)} |J, J_z-1\rangle. \end{aligned} \quad (30)$$

¹ How to solve this type equation are in Appendix VII.

Acting J_+ and J_- on all possible states to get the matrix elements:

$$J_+ |1, -1\rangle = \sqrt{2} |1, 0\rangle$$

$$J_+ |1, 0\rangle = \sqrt{2} |1, 1\rangle$$

$$J_+ |1, 1\rangle = 0$$

We can obtain a set of similar relations for J_- . Obtaining the matrix form of the operators:

$$\begin{aligned} J_z &= \begin{bmatrix} -1 & 0 & 0 \\ 0 & 0 & 0 \\ 0 & 0 & 1 \end{bmatrix} \\ J_+^2 &= \begin{bmatrix} 2 & 2 & 0 \\ 2 & 2 & 0 \\ 0 & 0 & 0 \end{bmatrix} \\ J_-^2 &= \begin{bmatrix} 0 & 0 & 0 \\ 0 & 2 & 2 \\ 0 & 2 & 2 \end{bmatrix} \end{aligned} \quad (31)$$

Substitute back into Equation (29), we obtain

$$\begin{bmatrix} -\epsilon & 0 & v \\ 0 & 0 & 0 \\ v & 0 & \epsilon \end{bmatrix} \quad (32)$$

We now want to rewrite the Hamiltonian in terms of Pauli matrices,

$$\begin{aligned} J_z &= \sum_n j_z^{(n)} = \frac{1}{2}(Z_1 + Z_2) \\ \Rightarrow H_0 &= \epsilon J_z = \frac{\epsilon}{2}(Z_1 + Z_2) \\ H_1 &= \frac{1}{2}v(J_+^2 + J_-^2) \\ &= \frac{1}{2}V \left[\left(\sum_n j_+^{(n)} \right)^2 + \left(\sum_n j_-^{(n)} \right)^2 \right] \\ &= \frac{1}{2}v \left(\sum_{nm} \left(j_+^{(n)} j_+^{(m)} + j_-^{(n)} j_-^{(m)} \right) \right) \\ &= \frac{1}{2}v \sum_{nm} (j_x + i j_y)^{(n)} (j_x + i j_y)^{(m)} \\ &\quad + (j_x - i j_y)^{(n)} (j_x - i j_y)^{(m)} \\ &= \frac{1}{2}v \sum_{nm} (j_x^{(n)} j_x^{(m)} + i j_y^{(n)} j_x^{(m)} - j_y^{(n)} j_y^{(m)} \\ &\quad + j_x^{(n)} j_y^{(m)} - i j_y^{(n)} j_x^{(m)} - j_y^{(n)} j_y^{(m)}) \end{aligned} \quad (33)$$

Since

$$\begin{aligned} j_x &= \frac{X}{2} \\ j_y &= \frac{Y}{2} \\ j_z &= \frac{Z}{2} \end{aligned}$$

Equation (33) becomes

$$\begin{aligned} &v \sum_{nm} \left(j_x^{(n)} j_x^{(m)} - j_y^{(n)} j_y^{(m)} \right) \\ &= 2v \sum_{n < m} \left(\frac{X_n X_m}{2} - \frac{Y_n Y_m}{2} \right) \\ \Rightarrow H_1 &= \frac{1}{2}V(X_1 \otimes X_2 - Y_1 \otimes Y_2) \end{aligned} \quad (34)$$

Combining H_0 and H_1

$$H = \frac{\epsilon}{2}(Z_1 + Z_2) + \frac{1}{2}V(X_1 \otimes X_2 - Y_1 \otimes Y_2) \quad (35)$$

2. $J = 2$

Using again Equation (30), we obtain the Hamiltonian matrix for $J = 2$.

$$H_{J=2} = \begin{pmatrix} -2\epsilon & 0 & \sqrt{6}V & 0 & 0 \\ 0 & -\epsilon + 3W & 0 & 3V & 0 \\ \sqrt{6}V & 0 & 4W & 0 & \sqrt{6}V \\ 0 & 3V & 0 & \epsilon + 3W & 0 \\ 0 & 0 & \sqrt{6}V & 0 & 2\epsilon \end{pmatrix} \quad (36)$$

Since this case follows the same Hamiltonian, upon inspection, we can rewrite the Hamiltonian in terms of the quasispin operators now for the $J = 2$ case. Note that the H_0 is a one body term, we take all linearly combination of the Z and I , the identity operator with one Z , the X and Y terms both act on two bodies, so we need to take all combination of XX (or YY) and II . The tensor product \otimes sign is omitted for simplicity.

$$\begin{aligned} H &= \epsilon(ZIII + IZII + IIZI + IIIZ) \\ &\quad + \frac{v}{2}(XXII + XIXI + XIIX + IXXI + IXIX + IIXX) \\ &\quad - \frac{v}{2}(YYII + YIYI + YIIY + IYYI + IYIY + IYYI) \end{aligned} \quad (37)$$

Again, rewriting the Hamiltonian in terms of Pauli matrices allows us to perform quantum computation with them.

We could also rewrite H_2 in terms of the Pauli matrices. Since \hat{N} acting on any of the four qubit state must give $4|\psi\rangle$, we can represent it $4IIII$. The second term can be rewritten in similar ways to H_1

$$\begin{aligned} \Rightarrow H_2 &= \frac{1}{2}W(4IIII + 2(XXII + \dots IIXX \\ &\quad + YYII \dots IYYI)) \end{aligned}$$

D. Variational Quantum Eigensolver (VQE)

The Variational Quantum Eigensolver (VQE) is a quantum algorithm that employs a hybrid approach,

combining quantum and classical processes, in order to find the ground state energy of a Hamiltonian. This algorithm is based on the Variational Principle, which states that the expectation value of the Hamiltonian, evaluated in any state, will always be greater than or equal to the ground state energy [4].

Mathematically,

$$E(\vec{\theta}) = \langle \Psi(\vec{\theta}) | \hat{H} | \Psi(\vec{\theta}) \rangle \geq E_0 \quad (38)$$

where $|\Psi(\vec{\theta})\rangle$ is any state of a quantum system parameterised by a set of parameters $\vec{\theta}$, \hat{H} is the Hamiltonian operator of the system and E_0 is the ground state energy.

The VQE algorithm follows these steps:

1. Prepare a parameterised quantum circuit (the ansatz) $|\Psi(\vec{\theta})\rangle$.
2. Measure the expectation value $E(\vec{\theta})$.
3. Use a classical optimization algorithm (gradient based or not) to update the parameters $\vec{\theta}$.
4. Repeat the above steps until the change in $E(\vec{\theta})$ is below a certain threshold.

f

Unlike some of the other quantum algorithms, such as the quantum phase estimation algorithms (QPE), which is in theory more efficient, non-hybrid and non-variational but only applicable to large-scale fault tolerant quantum computers, VQE is viable in the current Noisy Intermediate-Scale Quantum (NISQ) computers [5, 6].

III. METHODS

A. Level Mapping

The fermions in the lipkin model needs to be mapped to qubits. One way, perhaps the more natural way, to map the fermions is by using one qubit to represent a state (n, σ) where n is the particle slot and σ is the level (either spin up or down). In this mapping it requires $2N$ qubits to represent a system of N particles since there are 2 levels.

However, we know also that the Lipkin model do not permit the shift between particle slots, hence given an n , it's not possible that both σ 's to be occupied at the same time. By taking advantage of this situation, we could consider the “level mapping”, where we associate a qubit with a doublet, with

$$\begin{aligned} |0\rangle &\longleftrightarrow |n, -1\rangle \\ |1\rangle &\longleftrightarrow |n, +1\rangle. \end{aligned}$$

This allows us to map two states to one qubit, requiring only N qubits for a system of N particles. [5, 7]

B. Ansatz

In the context of VQE, “ansatz” refers to the parametrised quantum circuit which performs a pre-set set a operations, with certain unbound parameters. There is no unique ansatz, however the choice of ansatz can be vital to the accuracy and efficiency of the algorithms.

If Rx and Ry represent the rotation gate in the x and y direction respectively, and θ, ϕ represent the angle arguments within domain $[-\pi, \pi]$ they take: for the one qubit model, the ansatz we used is:

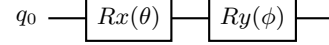


FIG. 1. One-qubit ansatz

For the two-qubit case, we used The CNOT gate at

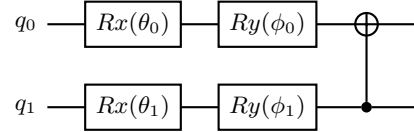


FIG. 2. Two-qubit ansatz

the end entangles the two qubit.

The four-qubit ansatz is: Although, in general, the

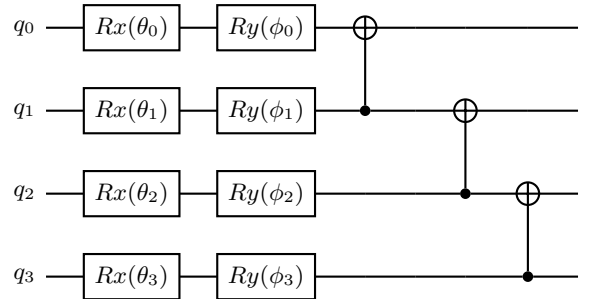


FIG. 3. Four-qubit ansatz

ground state will be a superposition of the state with all quasispins down and all states with any number pairs of quasispins flipped up. Therefore it is also possible to reduce the cost of preparing a variational state and requiring only a single variational parameter due to the parity symmetry [7].

C. Measurements

As mentioned in Section II A, our computational basis is in the Z basis, and by extension the ZI and $ZIII$ basis

etc. in higher dimensions. Therefore, in order to obtain the correct result for the other basis, we must rotate our circuit before taking measurements to the respective basis. This follows:

$$\begin{aligned} X &= HZH. \\ Y &= HS^\dagger ZHS \end{aligned} \quad (39)$$

For example, if one were to measure in the $XIXI$ basis, one must apply the Hadamard gate on the 0th and 2nd qubit to rotate the system to the $XIXI$ basis. Note that measurement destroys the state and therefore a copy of the state must be obtained before each change of basis. To obtain the correct coefficients, we need to repeat each measurement N times, with N sufficiently large. The measurement result is then the total number of counts divided by the number of shots, following

$$P(|\psi\rangle \rightarrow |x\rangle) \approx \sum_{n=0}^N \frac{x_n}{n} \quad (40)$$

For a precision of ϵ it requires $\mathcal{O}(1/\epsilon^2)$ samples for a circuit with depth $\mathcal{O}(1)$ [5].

IV. RESULTS

Each result was produced by running different eigen-solvers (both numerical and the VQE) for 100 different interaction strength (λ or v). When expectation values are calculated by taking repeated measurements, the number of shots was 10000 per measurement.

A. One Qubit

Figure 4 presents the simulation results for a single qubit system, comparing these results with those obtained from numerical calculations. The upper part of the figure presents the eigenvalues calculated using classical eigenvalue solvers as a function of the interaction strength (λ). Different colours represent distinct energy levels. It's important to clarify that these colours don't correspond to specific states but rather to the energy levels themselves.

The lower part of the figure displays the ground state energy determined using the VQE method for the one-qubit system, as calculated from both our custom implementation and the Qiskit library. The ground state energy is plotted against the interaction strength, which varies from 0 to 1 ($\lambda \in [0, 1]$).

B. Two Qubits

Figures 5 and 6 present results for a two-qubit system.

Specifically, Figure 5 demonstrates the simulation results obtained from our two-qubit system. The upper

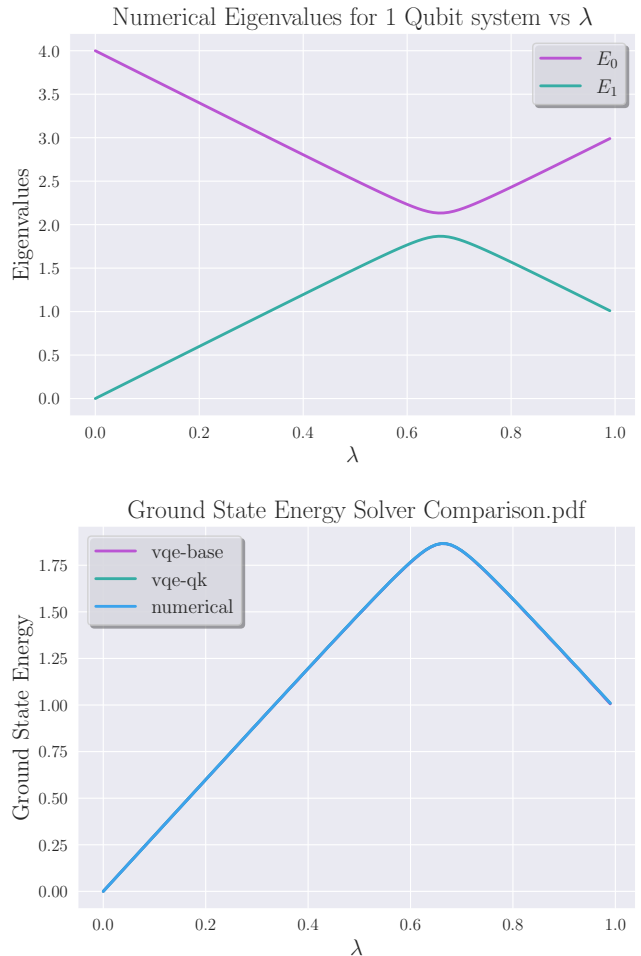


FIG. 4. Top: Classical eigenvalues as a function of the interaction strength λ , with colors denoting different energy levels. Bottom: Ground state energy calculated using VQE for a one-qubit system as a function of λ , from both our implementation and Qiskit.

part of the figure shows the numerical eigenvalues. Again, the different colours represent the distinct energy levels, not specific states. The lower part shows the ground state energy computed with the VQE method, using both our own implementation and the Qiskit library. Figure 6, on the other hand, shows the Von Neumann entropy for the ground state of our two-qubit system. The calculation of entropy allows us to understand the degree of entanglement in the ground state, offering insights into the complexity of the quantum state.

C. Lipkin Model: $J=1$

Figure 7 presents both numerical and simulation results for the Lipkin Model with $J = 1$. The upper plot shows the numerical results, while the lower plot illustrates the eigenvalues determined using the VQE

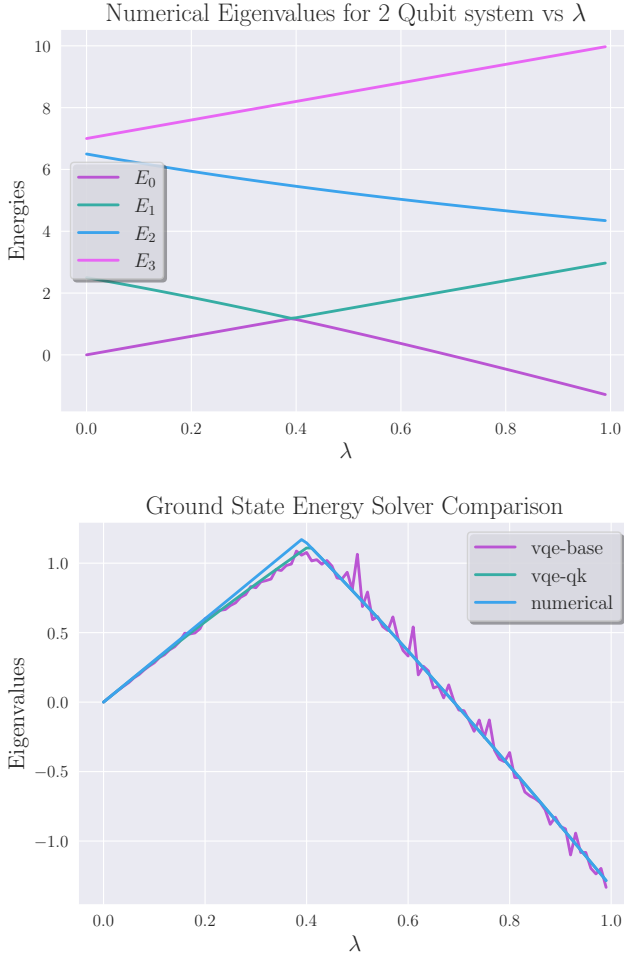


FIG. 5. Top: Numerical eigenvalues for a two-qubit system, with colors indicating distinct energy levels. Bottom: Ground state energy determined with VQE for a two-qubit system as a function of interaction strength λ , from both our implementation and Qiskit. .

method. This part of the study involves comparing results from both our custom implementation and the Qiskit library. The eigenvalues are plotted against the interaction strength parameter ($\frac{v}{\epsilon}$).

D. Lipkin Model: $J=2$

Finally, Figure 8 showcases the numerical and simulation results for the Lipkin Model with $J = 2$. The upper plot depicts the numerical results using the full Hamiltonian with a size of 16×16 . It's noteworthy that all of the energies possess degeneracy of 2. The lower plot shows the ground state energy for the Lipkin model for different values of interaction strength parameter $\frac{v}{\epsilon}$ for $\epsilon = 1$ and $v \in [0, 2]$, using an ansatz of depth 2.

Each result contributes to our overall understanding of the behaviour and characteristics of these quantum sys-

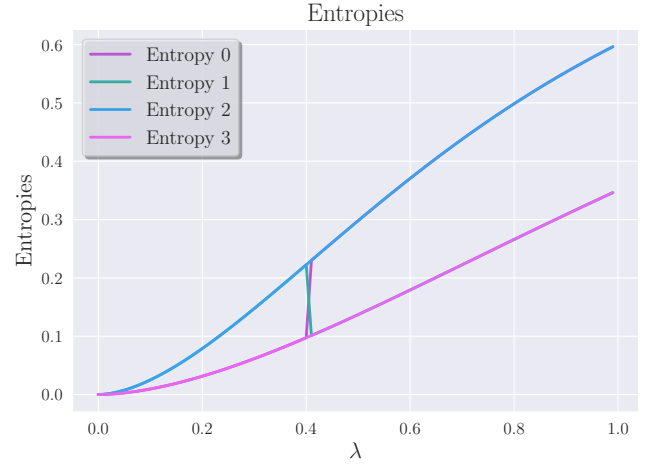


FIG. 6. Von Neumann entropy of the ground state for a simple two-qubit system as a function of interaction strength.

tems, and how effectively VQE can be used to simulate these systems and predict their properties. Further investigation and improvements can be made based on these initial findings to enhance the precision and efficiency of quantum simulations.

V. DISCUSSION

The implementation of a general N qubit quantum computer simulator is difficult, especially for multi-qubit gates that needs to take into consideration all possible combinations and generalised the matrix (operator) accordingly. The general N qubit class *Qubits* finds the corresponding indices for certain gates, specifically the CNOT and SWAP gates, instead of making a general N qubit operator. This has proven to be effective.

For the VQE methods, we chose not to implement our own minimisation methods since we noticed the gradient based methods from 'Qiskit' (ADAM) is a lot slower than the non-gradient based methods, (Sequential Least Squares Programming (SLSQP), Constrained Optimization BY Linear Approximations (COBYLA)). The classical optimisation was therefore done using functionalities from 'Scipy.optimize.minimize'.

For the one qubit case, as seen in Figure 4, all three methods produced results that are next to identical. For the two qubit system, both VQE methods produced good results. However, the VQE method from Qiskit had more point for which it failed to find the correct ground state (for multiple runs) but gave a more precise result when it does, while the VQE of our implementation created more 'bumps'. Given that the bumps seem to be uniformly distributed around the correct value, we can reasonably assume that it is caused by the errors from measurement when calculating the expectation values.

Indeed, when increase the number of shots to 100000,

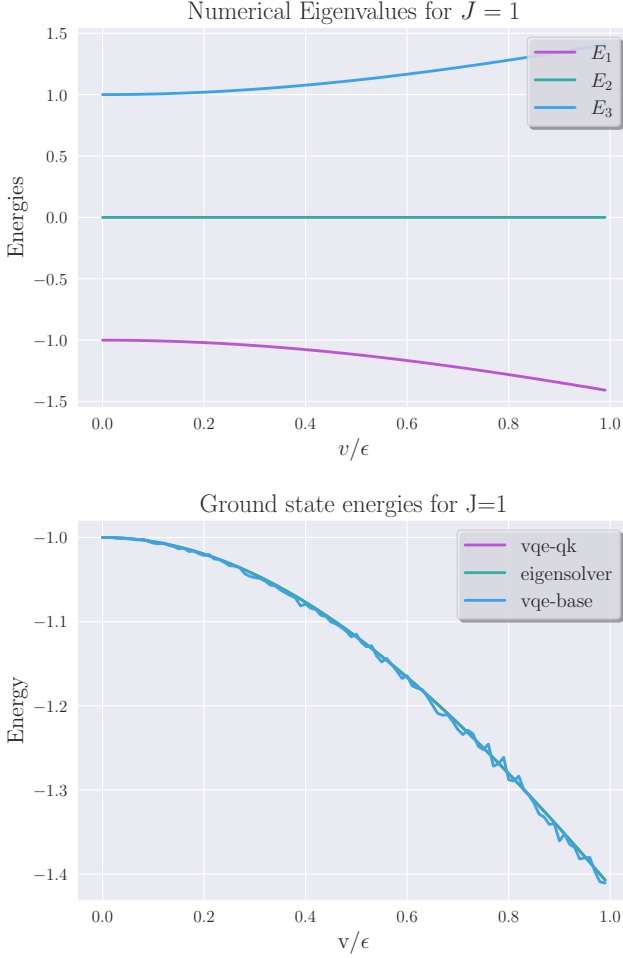


FIG. 7. Top: Numerical results for the Lipkin Model with $J = 1$. Bottom: Eigenvalue computed using VQE for the Lipkin Model with $J = 1$ as a function of interaction strength $\frac{v}{\epsilon}$, from both our implementation and Qiskit.

the ‘bumps’ smoothed out (Figure 10), but the circuit ran relatively slowly, therefore they are not repeated for more complicated circuits. The Von Neumann entropy of the ground state is also interesting, we see a general increase in entropy as interaction strength increases which aligns with our expectations, and at the level crossing we see a huge leap of the entropy, signifying a drastic increase in entanglement.

The inclusion of the final CNOT gate in the ansatz as shown in Figure 2 was essential as it introduced entanglement to the circuit, the results obtained without the CNOT gate were not impressive, as in Figure 9. The circuit was able to predict the ground state before the level crossing, but both failed and converged to an incorrect state afterwards.

The results for the $J = 1$ have performance similar to the simple two qubit system, with less failed points from the Qiskit VQE. For $J = 2$ however, both the VQE meth-

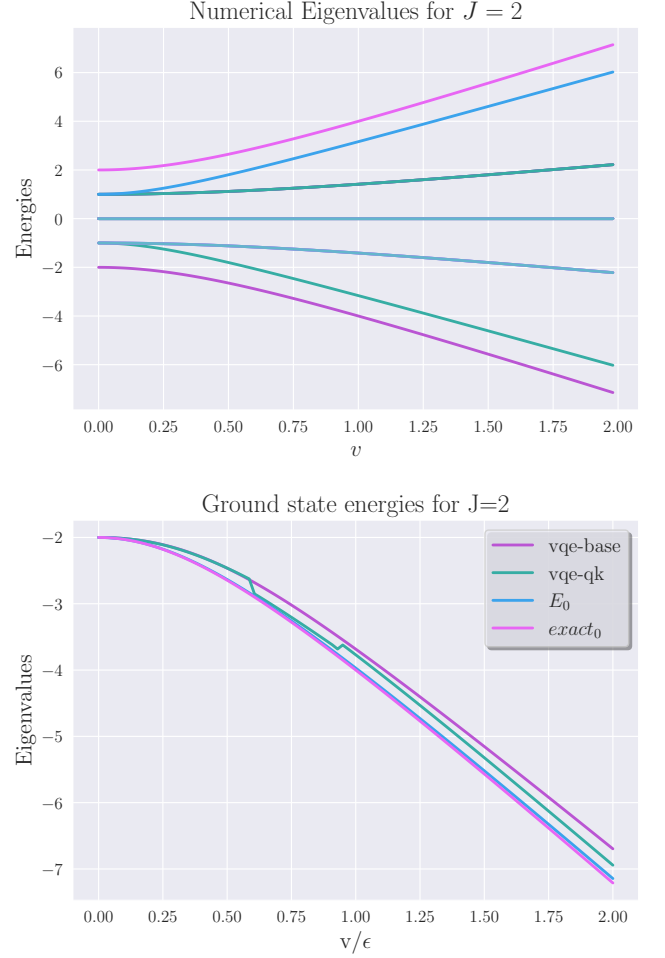


FIG. 8. Top: Numerical results for the Lipkin Model with $J = 2$, utilising the full Hamiltonian with size 16×16 , where all energies have a degeneracy of 2. Bottom: Ground state energy of the Lipkin model as a function of $\frac{v}{\epsilon}$ for $\epsilon = 1$, using an ansatz with depth 2.

ods from Qiskit and our own had some visible discrepancies from the exact value. Even the numerical eigenvalue solver wasn’t able to obtain the result with high enough accuracy, as seen in Figure 8. We failed to compute the expectation value correctly, despite following the same procedure as section III C. This figure contained results from computing the expectation values exactly by taking:

$$\langle \psi | H | \psi \rangle$$

This could be a result of unwise choice of ansatz, however, this ansatz gave the best results amongst many others which included more CNOT gates for non-neighbouring qubits or Toffoli (CCNOT) gate(s). One could also consider using an Hartree Fock ansatz [8]. Since the numerical eigenvalue solver underperformed in this task, it could also be simply due to the complexity of the problem or the lack of computational power, which could potentially be improved by setting a lower tolerance rate or increase

the maximum iteration steps.

Another possibility is the parameters' initialisation. One could try initialising using pre-trained parameters which might improve the performance.

VI. CONCLUSION

Throughout this study, we have delved into the investigation of the Lipkin model with the Variational Quantum Eigensolver (VQE) method, implemented in a simulated quantum computing environment. We started with a simple one and two-qubit model and then for more complex models, specifically focusing on a Lipkin model.

Our implementation demonstrated the potential of such a hybrid algorithm in solving many body physics problems. Both the VQE methods, one from Qiskit and our own, delivered compelling results for the one and two qubit simple cases. Despite certain inconsistencies in the two-qubit systems, both the simple and Lipkin, our implementation achieved a performance comparable to that of Qiskit.

However, the results for $J = 2$ showed some discrepancies from the exact value and the expectation value calculation appears to be faulty. This could be attributed to multiple factors like the choice of ansatz or the initialisation of parameters. Adjustments in these aspects may improve the accuracy of the results.

For future work, improvements could be made in all aspects. Perhaps the most obvious choice being extending the VQE study to include the H_2 term in the Lipkin model and exploring different ansatzs using the parity symmetry mentioned in papers [7]. On top of that, our base quantum computer simulator could be improved to include a generic function to rotate the basis. This would eliminate the need for setting up an expectation value each time we use a different Hamiltonian, reduce the likelihood of introducing errors.

In summary, our study again showed the promising potential for the Variational Quantum Eigensolver. Despite requiring refinements, our understanding in quantum computing and the VQE method has deepened. We believe this will act as a stepping stone for future work.

VII. APPENDIX A: REWRITE A MATRIX IN TERMS OF ANOTHER ABSIS

1. Consider the general 4x4 matrix M:

$$M = \begin{bmatrix} m_{11} & m_{12} & m_{13} & m_{14} \\ m_{21} & m_{22} & m_{23} & m_{24} \\ m_{31} & m_{32} & m_{33} & m_{34} \\ m_{41} & m_{42} & m_{43} & m_{44} \end{bmatrix}$$

2. Express the tensor products of I and σ_z :

$$M = (a \cdot I \otimes I) + (b \cdot I \otimes \sigma_z) + (c \cdot \sigma_z \otimes I) + (d \cdot \sigma_z \otimes \sigma_z)$$

$$I \otimes I = \begin{bmatrix} 1 & 0 & 0 & 0 \\ 0 & 1 & 0 & 0 \\ 0 & 0 & 1 & 0 \\ 0 & 0 & 0 & 1 \end{bmatrix}$$

$$I \otimes \sigma_z = \begin{bmatrix} 1 & 0 & 0 & 0 \\ 0 & -1 & 0 & 0 \\ 0 & 0 & 1 & 0 \\ 0 & 0 & 0 & -1 \end{bmatrix}$$

$$\sigma_z \otimes I = \begin{bmatrix} 1 & 0 & 0 & 0 \\ 0 & 1 & 0 & 0 \\ 0 & 0 & -1 & 0 \\ 0 & 0 & 0 & -1 \end{bmatrix}$$

$$\sigma_z \otimes \sigma_z = \begin{bmatrix} 1 & 0 & 0 & 0 \\ 0 & -1 & 0 & 0 \\ 0 & 0 & -1 & 0 \\ 0 & 0 & 0 & 1 \end{bmatrix}$$

3. Set up a system of equations by equating the corresponding elements of M and the tensor product combinations:

$$m_{11} = a + b + c + d$$

$$m_{12} = 0$$

$$m_{13} = \dots$$

$$\dots$$

4. Solve the system of equations to find the values of the coefficients a, b, c and d.

By determining the specific values of the coefficients a, b, c, and d, we can then rewrite any 4x4 matrix in the form:

$$M = (a \cdot I \otimes I) + (b \cdot I \otimes \sigma_z) + (c \cdot \sigma_z \otimes I) + (d \cdot \sigma_z \otimes \sigma_z)$$

VIII. APPENDIX B: OTHER RESULTS

-
- [1] J. Tilly, H. Chen, S. Cao, D. Picozzi, K. Setia, Y. Li, E. Grant, L. Wossnig, I. Rungger, G. H. Booth, and et al., *Physics Reports* **986**, 1–128 (2022).
- [2] M. Q. Hlatshwayo, Y. Zhang, H. Wibowo, R. LaRose, D. Lacroix, and E. Litvinova, *Physical Review C* **106** (2022),

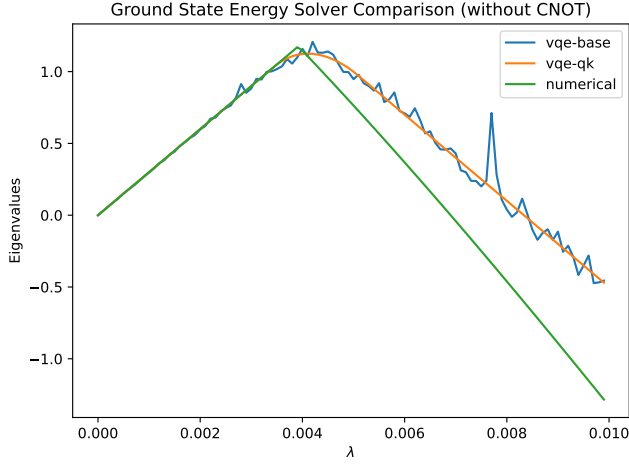


FIG. 9. Two Qubit results without CNOT gate in the sansatz.

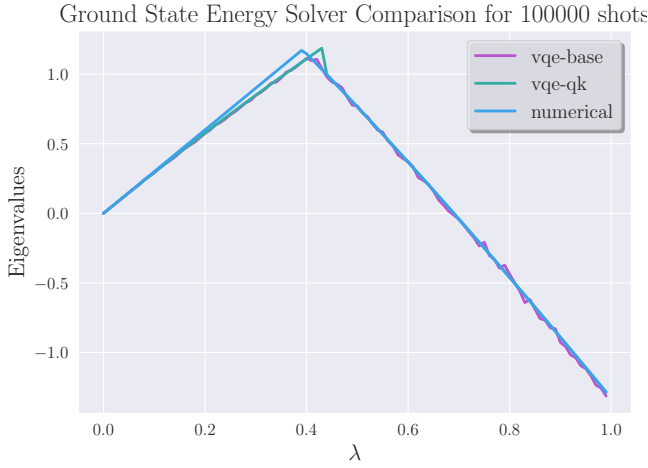


FIG. 10. Two qubit system with 100000 shots.

[10.1103/physrevc.106.024319](https://arxiv.org/abs/10.1103/physrevc.106.024319).

- [3] H. Lipkin, N. Meshkov, and A. Glick, *Nuclear Physics* **62**, 188–198 (1965).
- [4] M. A. Nielsen and I. L. Chuang, *Quantum Computation and Quantum Information* (Cambridge University Press, 2000).
- [5] CompPhysics, “[Quantumcomputingmachinelearning/week8.ipynb](#) at [gh-pages](#) · [compphysics/quantumcomputingmachine-learning](#),” .
- [6] J. Preskill, *Quantum* **2**, 79 (2018).
- [7] M. J. Cervia, A. B. Balantekin, S. N. Coppersmith, C. W. Johnson, P. J. Love, C. Poole, K. Robbins, and M. Saffman, *Physical Review C* **104** (2021), [10.1103/physrevc.104.024305](https://arxiv.org/abs/10.1103/physrevc.104.024305).
- [8] D. A. Fedorov, B. Peng, N. Govind, and Y. Alexeev, *Materials Theory* **6** (2022), [10.1186/s41313-021-00032-6](https://arxiv.org/abs/10.1186/s41313-021-00032-6).

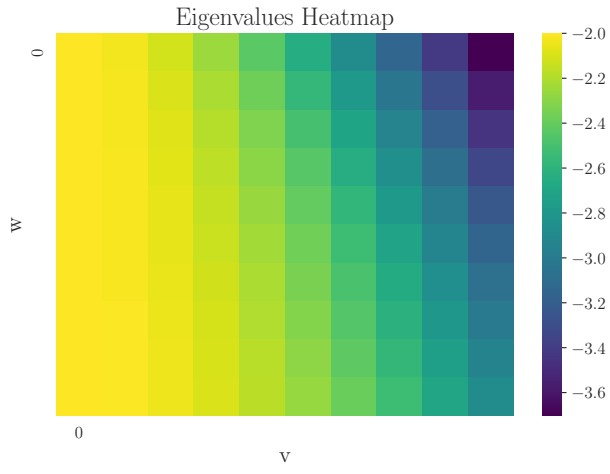


FIG. 11. Ground state energy eigenvalue obtained by classical eigensolver with H_2 , for $v \in [0, 1], w \in [0, 1]$